

# Influence of the dislocation density on hardening precipitation in Inconel© 625

Anthony SERET<sup>a</sup>, Charbel MOUSSA<sup>a</sup>, Marc BERNACKI<sup>a</sup>, Jonathan CORMIER<sup>b</sup>,  
Nathalie BOZZOLO<sup>a</sup>

<sup>a</sup> CEMEF – Centre de mise en forme des matériaux, Mines ParisTech, PSL – Research University, CNRS UMR 7635, CS 10207 rue Claude Daunesse 06904 Sophia Antipolis Cedex, France

<sup>b</sup> Institut Pprime – Université de Poitiers – ENSMA, Physics and Mechanics of Materials Department, Chasseneuil, France

## Abstract

Inconel© 625 is a Nickel-base superalloy used in aerospace industry as turbine shrouds, spray bars, hydraulic tubing, armoring and thrust reversers systems [1]. One reason of its use is its high mechanical properties at high temperature. Inconel© 625 is strengthened by precipitation of  $\gamma''$  phase, tetragonal  $\text{Ni}_3\text{Nb}$  [1]. Since dislocations can influence precipitation [2], the precipitation of  $\gamma''$  in Inconel© 625 was studied in samples submitted to cold straining to induce different dislocation contents before precipitation heat treatment.

## Material and experimental procedure

Inconel© 625 was supplied by Safran Nacelles as 1 mm-thick sheet homogenized at 1038 °C @ 4 h. In order to study the influence of dislocations on  $\gamma''$  precipitation, samples were strained (up to 40 % by room temperature uniaxial tension) and submitted to an ageing treatment (650 °C@500 h + air cooling) that was previously demonstrated to be efficient in promoting  $\gamma''$  precipitation [1]. The as-received homogenized state was also submitted to the same treatment to serve as reference state with low dislocation content.

Dislocation content was estimated, before annealing, based on Electron Backscatter Diffraction (EBSD) maps acquired with a Zeiss SUPRA40 field emission gun scanning electron microscope (FEG-SEM) equipped with a Bruker EBSD e<sup>-</sup> Flash<sup>HR</sup> EBSD detector and the Esprit 2.1 software package. EBSD data were processed using the MTEX Matlab toolbox [3]. A density of geometrically necessary dislocations was estimated from the analysis of intragranular orientation gradients following a principle inspired from [4] and [5] to reduce the measurement noise bias, but where the kernel average misorientation was replaced by the curvature tensor.

After annealing, high magnification images of  $\gamma''$  precipitates were recorded using the InLens secondary electron (SE) detector of the SUPRA 40 FEG-SEM. In order to reveal fine precipitation, the samples were prepared by mechanical polishing and etching: automatic rotative polishing with abrasive SiC papers, followed by electropolishing 45 V @ 4 s in (90 % volume methanol + 10 % volume perchloric acid) electrolyte. Image analysis was then performed to retrieve quantitative parameters describing precipitation topology: mean intercept length (all possible lines), volume fraction and number of

precipitates per unit area. Images were recorded at  $\times 100k$  magnification, 8 and 10 images were analyzed, providing 4732 and 6203 precipitates for unstrained and strained samples, respectively.

## Results

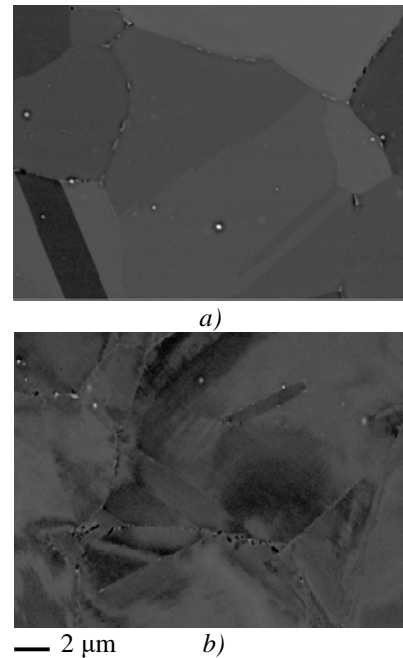


Figure 1: SEM backscattered electron (BSE) images providing orientation and chemical contrast of aged samples (500 h @ 650 °C)  
a) no pre-strain b) 40 % pre-strain

Figure 1 shows the microstructures of the unstrained and of the 40% pre-strained samples after ageing treatment. As expected, the unstrained sample has grains of uniform crystal orientation, while grains of the 40 % strained sample exhibit a BSE contrast typical for deformed microstructures with heterogeneous crystal orientation and local plastic strain structures like slip planes.

Table 1: mean GND density vs. applied pre-strain

pre-strain [%]	0	10	20	30	40
GND density [ $10^{14} \text{ m}^{-2}$ ]	0.46	0.86	2.7	4.4	5.0

Table 1 shows the values of the mean GND density measured in samples as function of pre-strain. The unstrained and the 40 % pre-strained samples differ by one decade on the mean GND density.

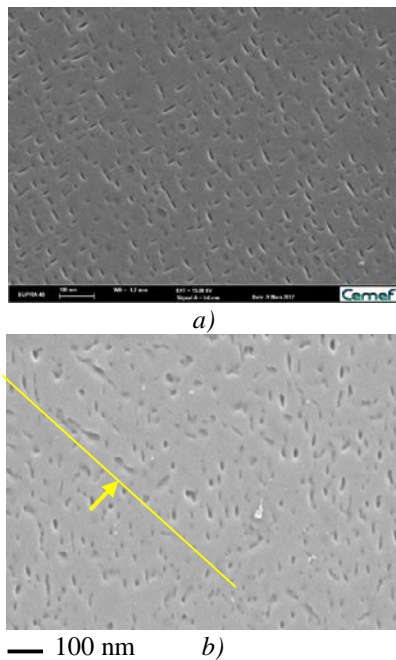


Figure 2: SEM secondary electron image providing the  $\gamma''$  phase topology in aged samples (500 h @ 650 °C)  
a) no pre-strain b) 40 % pre-strain

Figure 2 shows the  $\gamma''$  phase topology in the unstrained and in the 40% pre-strained samples after ageing treatment. The  $\gamma''$  precipitates differ in shape and to some extent in size. The  $\gamma''$  precipitates appear ellipsoidal along three typical directions in the 2D section of the unstrained state (agrees with [6]) and have less regular shapes and orientation in the pre-strained sample. This suggests that during nucleation and growth in the strained  $\gamma$  matrix,  $\gamma''$  precipitates conserved the  $\gamma$ - $\gamma''$  orientation relationship as previously shown in Inconel 718 [2,6]. Moreover, in the strained state,  $\gamma''$  precipitates, albeit ellipsoidal, seem closer to spherical than in the unstrained state, which was also observed on rolled Inconel© 718 [2]. In the unstrained state  $\gamma''$  precipitates are elongated along 3 directions due to orientation relationship with  $\gamma$  matrix [6]; in the strained state they are randomly oriented. Crystal orientation is heterogeneous in grains of the strained state, so  $\gamma''$  random morphological orientation agrees with the assumption that  $\gamma$ - $\gamma''$  orientation relationship holded during nucleation and growth. In both samples, precipitates are rather regularly spaced, however the strained state seems to present alignments of a few  $\gamma''$  precipitates (arrowed on Fig. 2b), which could be related to a preferential nucleation along slip planes.

The size of the precipitates has been quantified by mean intercept length (Fig. 3a) : 6.1 nm and 6.5 nm for the unstrained and pre-strained samples, respectively. The  $\gamma''$  volume fraction is also higher in the strained state (Fig. 3b) : 4.9% and 5.6% for the unstrained and pre-strained samples, respectively. This may come from dislocations acting as high-diffusivity paths for Nb atoms from matrix to  $\gamma''$ , feeding  $\gamma''$  growth. The number of precipitates per

area unit are  $6.65 \cdot 10^2 (\mu\text{m})^{-2}$  and  $7.14 \cdot 10^2 (\mu\text{m})^{-2}$  for the unstrained and strained samples, respectively, suggesting that dislocations also promoted  $\gamma''$  nucleation.

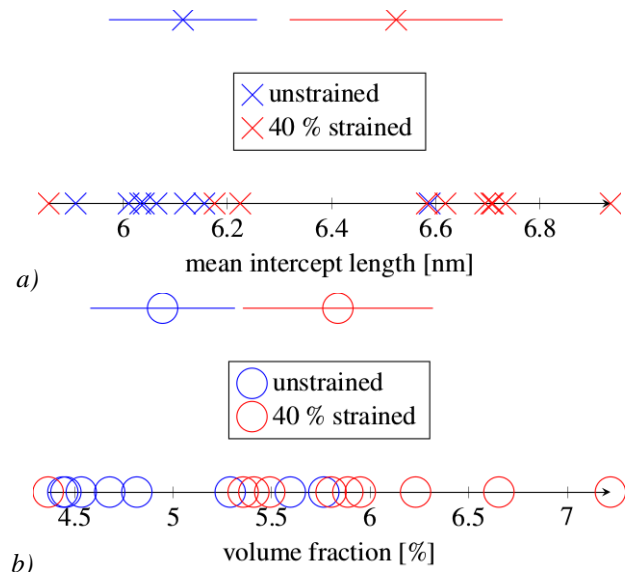


Figure 3: a) mean intercept length and b) volume fraction of  $\gamma''$  precipitates in the unstrained and 40 % pre-strained samples, after ageing for 500 h @ 650 °C.

Bottom: values of each analyzed image; top: average value of all images and 95 % confidence interval

Different volume fraction suggest that coarsening at equilibrium constant volume fraction is not reached, but growth is still in course after 500h @ 650 °C. This is supported by Thermo-Calc calculations indicating a  $\delta$  phase equilibrium volume fraction of 11.1 % ( $\delta$  is the stable version of  $\gamma''$ , same chemistry).

## Conclusions

By comparing the  $\gamma''$  precipitation in the Inconel© 625 Nickel base superalloy after 500h @ 650°C, with or without a pre-strain, it could be confirmed that dislocations, as expected, promote nucleation and growth of precipitates by acting as diffusion short-paths, but affect also the shape and orientation of precipitates. The strained material exhibits more spherical precipitates with more random morphological orientation.

## Acknowledgements

This work has been carried out within the frame of the ANR-Safran industrial chair OPALÉ.

## References

- [1] L. Mataveli Suave *et al.*, *MATEC Web of Conferences*, 14 (2014) 21001
- [2] Y. Mei *et al.*, *Journal of Alloys and Compounds*, 649 (2015) 949–960
- [3] F. Bachmann *et al.*, *Solid State Phenomena* 160 (2010) 63–68
- [4] C. Moussa *et al.*, *Ultramicroscopy* 179 (2017) 63–72
- [5] M. Kamaya, *Ultramicroscopy*, 111 (2011) 1189–1199
- [6] A. Niang, PhD thesis, Institut national polytechnique de Toulouse, 2010.